BULLETIN OF THE POLISH ACADEMY OF SCIENCES
TECHNICAL SCIENCES, Vol. 67, No. 3, 2019
DOI: 10.24425/bpasts.2019.129662

Hydrides precipitation in Ti6Al4V titanium alloy used for airframe manufacturing

D.I. BĂILĂ* and S. TONOIU

Politehnica University of Bucharest, Blv. Splaiul Independentei, No. 313, sector 6, 060042 Bucharest, Romania

Abstract. The aeronautical industry is a sector constantly looking for new materials and equipment because of its tendency to expand quickly. The Ti6Al4V titanium alloy is used frequently in the aeronautic, aerospace, automobile, chemical and medical industry because it presents high strength combined with low density (approximately 4.5 g/cm^3), good creep resistance (up to 550°C), excellent corrosion resistance, high flexibility, good fatigue and biocompatibility. As a result of these properties, this titanium alloy is considered an excellent material for manufacturing structural parts in the aircraft industry for modern aeronautic structures, especially for airframes and aero-engines. But its use is also problematic because the Ti6Al4V titanium alloy manifests hydrogen embrittlement, by means of hydrides precipitation in the metal. The Ti6Al4V alloy becomes brittle and fractures because of hydrogen diffusion into metal and because titanium hydrides appear and create pressure from within the metal, thus generating corrosion. Because of titanium hydrides, the titanium alloy suffers from reduced ductility, tensile strength and toughness, which can result in fractures of aeronautical parts. This poses a very serious problem for aircrafts. In this paper, rapid hydrogen embrittlement is presented along with XRD, SEM and TEM analysis. Its goal is to detect the presence of titanium hydrides and to spot the initial cracks in the metallic material.

Key words: hydrides precipitation, Ti6Al4V alloy, hydrogen embrittlement, pitting corrosion.

1. Introduction

In the aeronautical industry, the airframe of an aircraft contains the fuselage, the wings and the undercarriage. The airframe's design necessitates consideration of all of the following: manufacturing processes, materials technology, aerodynamics, performance and cost [1].

The Ti6Al4V titanium alloy is an important lightweight material used frequently in aerospace structures, which require high performance, excellent structural efficiency, good fatigue and excellent mechanical resistance. However, conventional manufacturing processes of the Ti6Al4V alloy entail high production costs because the titanium alloy is difficult to manufacture.

Previously, conventional processes have been replaced with additive laser manufacturing processes, such as SLS (selective laser sintering), DMLS (direct metal laser sintering), SLM (selective laser melting) and others. The additive laser manufacturing processes allow to produce low volume complex components and the time and costs involved are considerably lower [2, 3].

Titanium alloys are classified into four categories as concerns the function of their chemical composition and microstructure at room temperature. Thus they are divided into α alloys, α + β alloys, metastable β alloys and β alloys [4–6].

Ti6Al4V is an α + β alloy containing 6wt% aluminum stabilizing the α phase (for the improvement of strength and hardness) and 4wt% vanadium, which stabilizes the β phase (for the improvement of ductility and mechanical properties).

The Ti6Al4V alloy's microstructure at equilibrium and at room temperature consists predominantly of the α phase (hcp) with some retained β phase (bcc). The microstructure of this alloy depends of the cooling rate and it can take several different forms, such as grain boundary allotriomorph α, globular α as well as the Widmanstätten and martensitic ones.

The final microstructure of Ti6Al4V is significantly influenced by the β → α phase transformation.

Figure 1 presents the homogenous structure of the Ti6Al4V cast alloy, evidencing fine equiaxed α phase grains (dark gray)

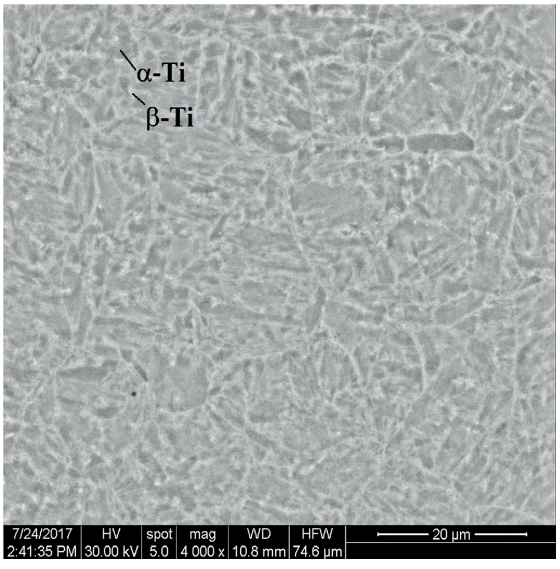

(X 4000)

Fig. 1. SEM analysis of Ti6Al4V cast alloy

*e-mail: baila_d@yahoo.com

Manuscript submitted 2018-10-06, revised 2019-01-06, initially accepted for publication 2019-01-29, published in June 2019.

and β phase grains (light gray), using SEM analysis to this end. The alloy composition and cooling rate influence the transformation from the bcc β to hcp α phase and can appear as a martensitic phase or as a diffusion-controlled nucleation and growth process [7–9].

With its high specific strength (the ratio between the ultimate strength and its low density stands at 4.43 g/cm^3) and its high corrosion resistance at high temperatures, the Ti6Al4V alloy is frequently used in the aeronautical industry for airframe structures and engines.

Hydrogen is a light and mobile gas, which can get delicate when attempting to highlighting it by means of spectrometry. It is therefore necessary to form titanium hydrides, which can be detectable [10, 11].

The hydrogenation-dehydrogenation process is a thermo-mechanical treatment, highly important for powder atomization used in the DMLS and SLM process in the medical and aerospace industry [12, 13].

Hydrogen solubility is obtained at high temperature. Hydrogen solubility into an α phase increases with temperature [12–14].

Hydrogen embrittlement into pure titanium is noted when the hydrogen percentage reaches between 125 and 200 ppm, at room temperature [12–14].

Other elements of the alloy also influence hydrogen solubility into different phases of titanium.

D.M. Wanderwalker remarked that the augmentation of 5.87% Al increases the solubility limit of hydrogen from 21 ppm to 250 ppm, at room temperature [15].

First principles calculation of Liang [13] reveals that the hydrogen concentration is very important for determining brittle/ductile behavior at Ti-H phases and densities of states determine that a bonding transition from mainly covalent to mainly metallic occurs for Ti-H phases once the H/Ti ratio reaches about 1/8.

Liang and Gong show that within the Ti-H system, there exist two types of TiH_x hydrides phases (δ and ε) and the intrinsic composition range of the $\delta \rightarrow \varepsilon$ transition is $1.5 \leq x \leq 2$. The $\delta \rightarrow \varepsilon$ and $\delta \rightarrow \gamma$ transitions are quite different from each other, i.e. mechanical instability causes the $\delta \rightarrow \varepsilon$ transition while internal symmetry breaking of cubic structures induces the $\delta \rightarrow \gamma$ transition [13].

The apparent increase of solubility results from deformations augmentation necessities for hydrides germination within the alloy in the presence of aluminum.

Miaoquan remarked that the δ hydride (TiH_2 phase) occurs in the hydrogenated Ti6Al4V titanium alloy when the hydrogen content is more than 0.3 wt%. Aluminum present in the solution augments the hydrogen activity [17].

Hydrogen is beta-stabilized and the solubility limit of hydrogen into β phase of titanium alloys is more significant that into the α phase.

San Martin [14], D.M. Wanderwalker [15] and Laptev [16] estimate that the solubility limit of hydrogen into beta phase is 1.32% at 300°C. It thus becomes obvious that this excellent solubility is metastable.

Olsson built an *ab initio*-based density thermodynamic models and described structural properties of titanium hydrides [18].

Gutelmacher observed the appearance of three different varieties of titanium hydrides (δ, γ, ε) present under room temperature within titanium-based alloys [19].

Muthukumar studied the metal hydrides initiation-based heating and cooling systems [20].

In this paper, were conducted SEM, XRD and TEM analysis to determine the titanium hydrides formation at room temperature within the Ti6Al4V alloy. We have used an experimental cathode charging system to this end.

Titanium hydrides can alter the mechanical properties and this aspect is of interest for the aerospace, automobile and medical industry.

2. Experimental part

Investigation of morphology and quantitative analysis of compacts were performed using the Quanta Inspect F scanning electron microscope (qualitative and quantitative analysis) equipped with an electron gun with field emission (FEG, field emission gun) with a resolution of 1.2 nm, and an energy dispersive (EDS) x-ray spectrometer with a resolution of 133 eV at MnK.

XRD analysis was performed using an X-ray diffractometer based on PAnalytical Empyrean characteristic CuKα radiation and wavelength of 1.541874. Spectrum acquisition was performed using Bragg-Brentano geometry.

The samples microstructure was detected using a Tecnai G2 F30 S-Twin (300 kV) transmission electron microscope equipped with an electron gun with field emission (FEG, field emission gun) with TEM resolution of 2Å.

3. Pitting corrosion behavior of Ti hydrides within Ti6Al4V alloy

Two density currents were used in this paper, with three samples in each experiment. Cathode charging is realized in the H_2SO_4 solution, 0.1 mol/l. The density currents used are: $J = 100$ mA/cm^2 and $J = 150$ mA/cm^2.

The samples of the Ti6Al4V alloy are immersed in the solution for 24, 48 and 72 hours. The chemical reaction is given by following formula:

$$Ti + H_2 \rightarrow TiH_2. \tag{1}$$

Samples 3 and 5 are immersed for 24 hours, samples 1 and 4 are immersed for 48 hours and samples 2 and 6 are immersed for 72 hours.

Figure 2 presents the cathode charging system schema used for experimental research presented in this paper. The six samples are cut on prismatic forms and then polished and cleaned with alcohol prior to immersion in the H_2SO_4(0.1 M) solution. Table 1 presents experimental data such as current density J[mA/cm^2], time t[h], the surface S[mm^2] that is immersed in the H_2SO_4 solution 0.1 M and intensity I[A], all used for experimental determinations.

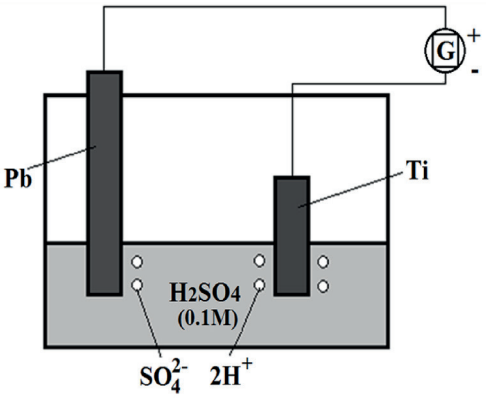

Fig. 2. Cathode charging system schema

Table 1
Samples of Ti6Al4V tested in the H_2SO_4 solution, 0.1 M

No.	Current density J[mA/cm^2]	Time t[h]	Surface S[mm^2]	Intensity I[A]
1	150	48	288.324	0.43
2	100	72	549.289	0.24
3	100	24	262.351	0.26
4	100	48	222.741	0.22
5	150	24	378.623	0.56
6	150	72	327.266	0.49

The XRD analysis for samples 1, 5 and 6 using current density J = 150 mA/cm^2 is presented in Figs 3, 4 and 5. Please note the α-Ti peaks (hexagonal close-packed) and β-Ti (body-centered cubic) for sample 5, as presented in Fig. 3. For sample 1, the peaks of titanium hydrides $TiH_{1.924}$ occur, as presented in Fig. 4.

As concerns sample 6, α phase titanium peaks disappear because of hydrogen diffusion in α-Ti, it being inserted in a solid solution. γ-TiH titanium hydrides then appear. The result is very interesting because this type of γ-TiH hydrides is usually not present alone.

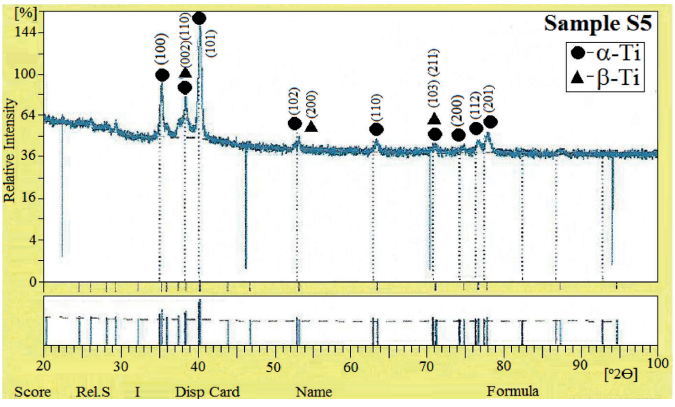

Fig. 3. XRD analysis for sample S5 immersed in H_2SO_4 (0.1M), using J = 150 mA/cm^2, during 24 hours

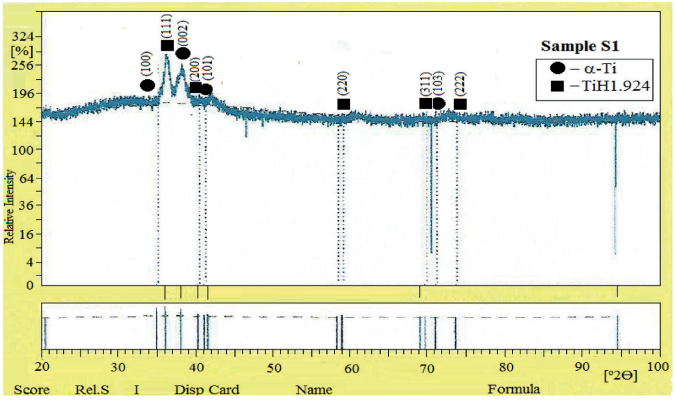

Fig. 4. XRD analysis for sample S1 immersed in H_2SO_4 (0.1M), using J = 150 mA/cm^2, during 48 hours

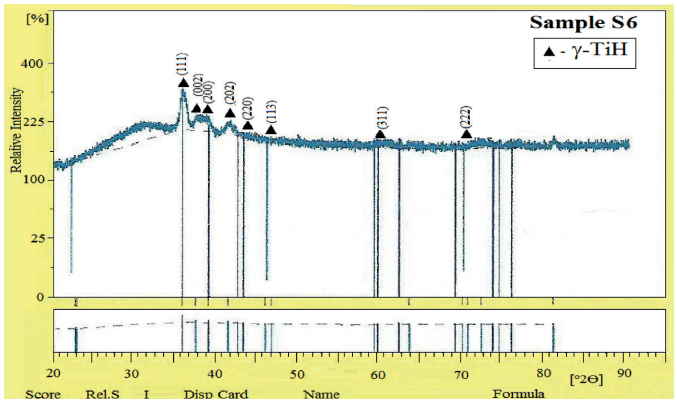

Fig. 5. XRD analysis for sample S6 immersed in H_2SO_4 (0.1M), using J = 150 mA/cm^2, during 72 hours

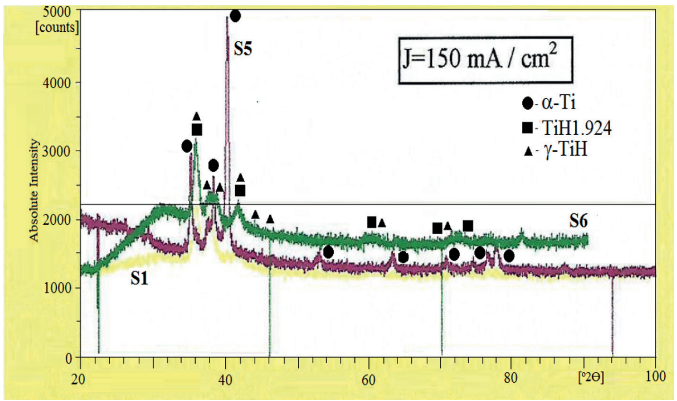

Fig. 6. Comparison between XRD analysis for samples S1, S5 and S6 immersed in H_2SO_4 (0.1 M), using J = 150 mA/cm^2

Figure 6 presents a comparison between XRD analysis for samples S5 (24 hours), S1 (48 hours) and S6 (72 hours) immersed in H_2SO_4 (0.1 M), using current density of J = 150 mA/cm^2. It can be noted that sample S6 presents increased corrosion, because of titanium hydride peaks apparition, unlike in sample S5.

The XRD analysis for samples 3, 4 and 2 using current density J = 100 mA/cm^2 is presented in Figs 7, 8 and 9. Regarding the XRD analysis, it can remarked that samples 3 and 4 present the peaks of hydride titanium TiH_2. XRD analysis for sample 2 shows the presence of TiH_2 and TiH and fine peaks can be noted. They tend to belong to the TiO_2 spectrum formed, most probably accidentally, in the case of favorable conditions for self-passivation of the Ti6Al4V alloy.

Figure 10 shows a comparison between XRD analysis for samples S3 (24 hours), S4 (48 hours) and S2 (72 hours) immersed in H_2SO_4 (0.1 M), using J = 100 mA/cm^2.

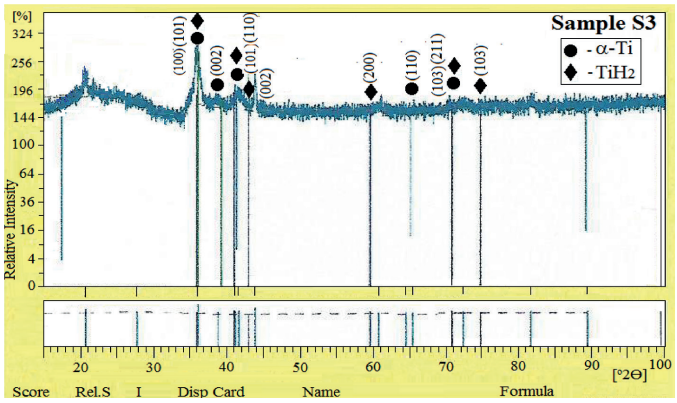

Fig. 7. XRD analysis for sample S3 immersed in H_2SO_4 (0.1 M), using J = 100 mA/cm^2, during 24 hours

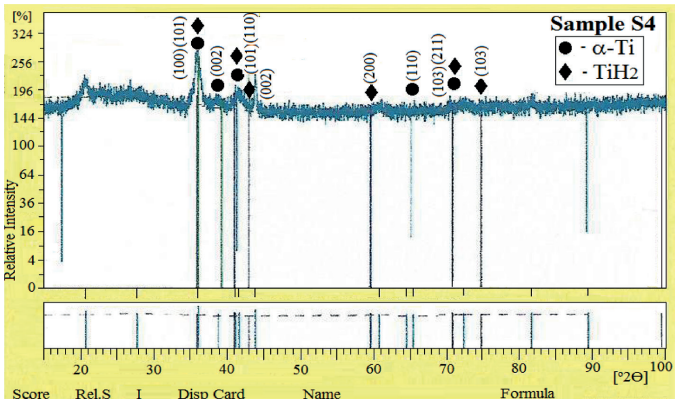

Fig. 8. XRD analysis for sample S4 immersed in H_2SO_4 (0.1 M), using J = 100 mA/cm^2, during 48 hours

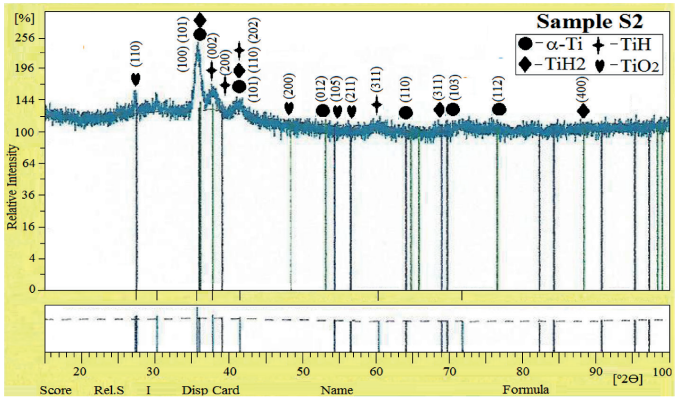

Fig. 9. XRD analysis for sample S2 immersed in H_2SO_4 (0.1 M), using J = 100 mA/cm^2, during 72 hours

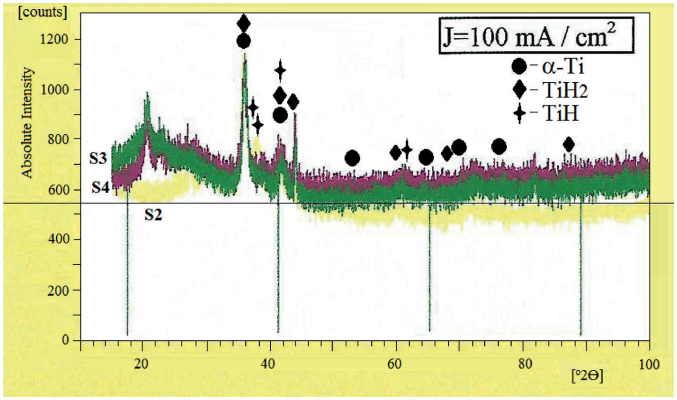

Fig. 10. Comparison between XRD analysis for samples S2, S3 and S4 immersed in H_2SO_4 (0.1M), using J = 100 mA/cm^2

The graphs are superposed and highlight the titanium hydrides appearance, especially $TiH_{1.924}$ (tetragonal phase), TiH_2 (tetragonal phase) and γ-TiH (tetragonal phase).

Titanium hydrides $TiH_{0.71}$ (orthorhombic phase), $TiH_{1.971}$ (cubic phase) and δ-TiH (orthorhombic phase) were not present in the XRD diagrams created in the course of this research.

In conclusion, in this paper we have provoked hydrides titanium precipitation using a cathode charging system. The XRD analysis determined the emergence in the Ti6Al4V alloy of different types of titanium hydrides, following immersion in H_2SO_4 (0.1 M).

Using TEM analysis, we have confirmed the occurrence of internal micro-cracks in the samples, such as those presented in Figs 11–16. Multiple crack initiation sites and multi-branched

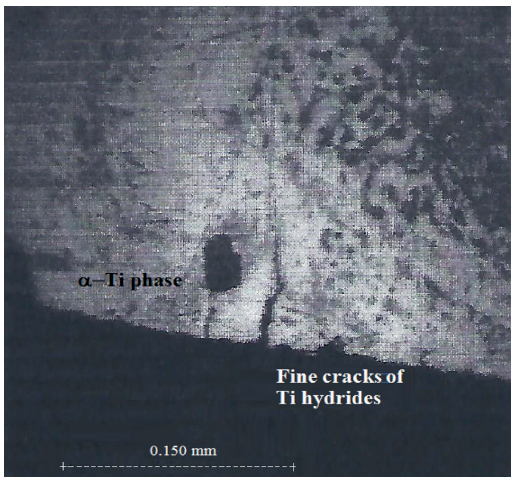

Fig. 11. Microstructure of sample S5 following immersion in H_2SO_4 (0.1M), using J = 150 mA/cm^2, during 24 hours

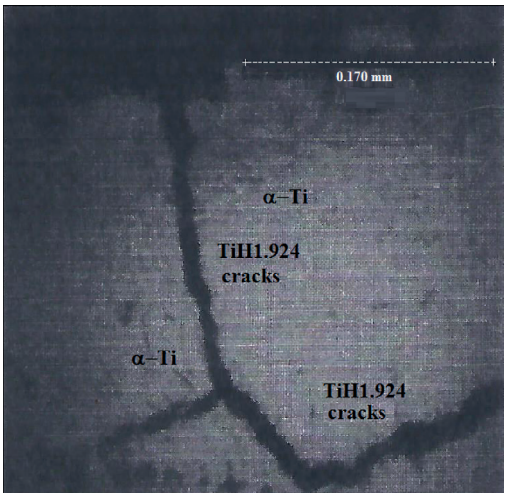

Fig. 12. Microstructure of sample S1 following immersion in H_2SO_4 (0.1 M), using J = 150 mA/cm^2, during 48 hours

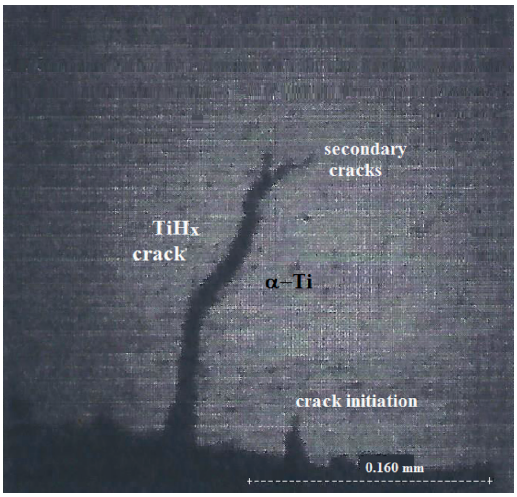

Fig. 13. Microstructure of sample S6 following immersion in H_2SO_4 (0.1 M), using J = 150 mA/cm^2, during 72 hours

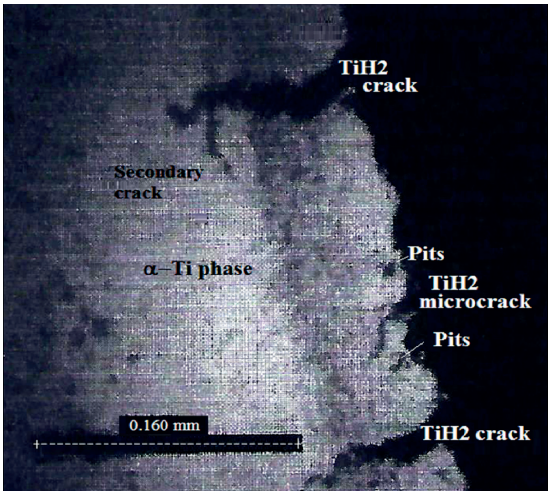

Fig. 14. Microstructure of sample S3 following immersion in H_2SO_4 (0.1 M), using J = 100 mA/cm^2, during 24 hours

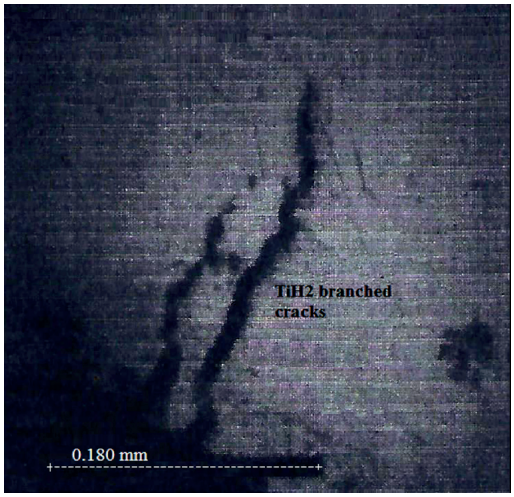

Fig. 15. Microstructure of sample S4 following immersion in H_2SO_4 (0.1M), using J = 100 mA/cm^2, during 48 hours

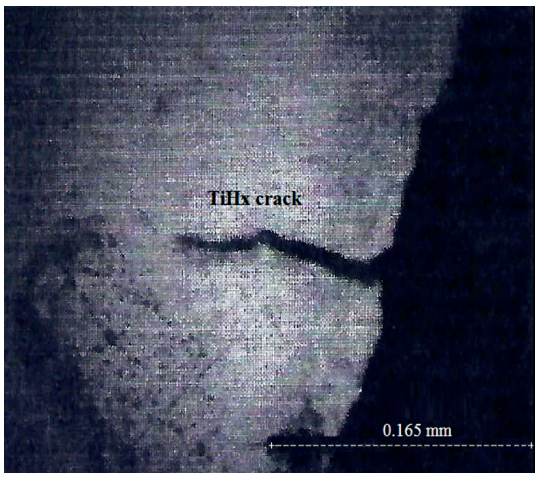

Fig. 16. Microstructure of sample S2 following immersion in H_2SO_4 (0.1 M), using J = 100 mA/m^2, during 72 hours

intergranular cracks on the inside of the samples, specific for pitting corrosion, can all be noted.

For sample 5, very fine cracks can be noted in the microstructure, such as those presented in Fig. 11. Titanium hydrides were undetected by XRD analysis for sample 5 because their quantity is very small, under 0.1%.

For samples 1 and 6, cracks and secondary cracks can be noted, because of the titanium hydrides formation and the accentuated corrosion phenomena, such as those presented in Figs 12 and 13. For sample 3 one can note fine cracks and pits in the titanium alloy, such as those presented in Fig. 14. When the time of immersion increases, one can observe the occurrence of long cracks in cross-section of the samples, caused by pitting corrosion, as in Figs 15 and 16.

It can be observed that the influence of current density increases the corrosion process. For J = 150 mA/m^2 the corrosion process is more intensive than for J = 100 mA/cm^2.

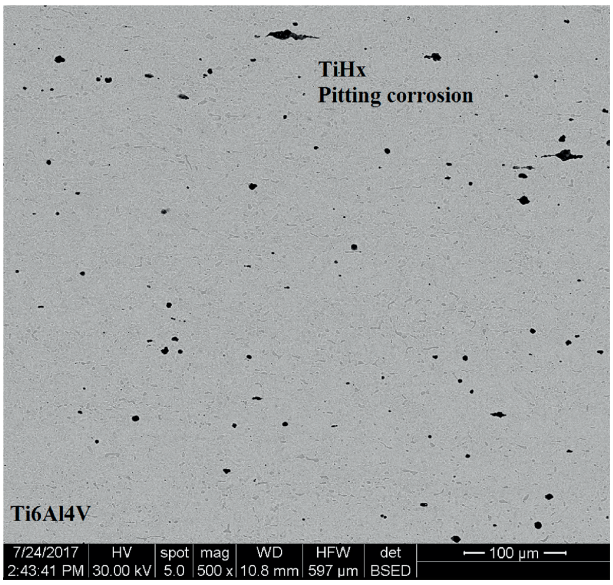

(X 500)

Fig. 17. SEM analysis of TiHx pitting corrosion on the Ti6Al4V alloy surface of sample S6

Because of the aggressive environment in which the experiment takes place (0.1 M sulfuric acid solution), there is a risk of spontaneous rupture of samples.

In Fig. 17, SEM analysis shows the pitting corrosion on the surface of sample S6, and the aggressive attack of titanium hydrides on the Ti6Al4V alloy can be noted. Cracking propagation processes are obtained by means of diffusion of hydrogen along the intergranular path and because of hydrogen accumulation it is favorable for hydrogen dislocations transport.

Figure 18 presents a propagation crack caused by hydrogen diffusion and the "mill annealed" structure of Ti6Al4V. Intergranular cracking propagation, between α phase grains and the hydrogen embrittlement, can be noted.

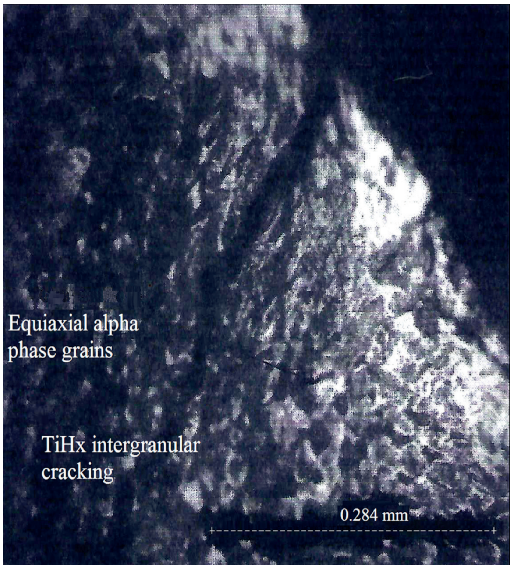

Fig. 18. Propagation of intergranular cracking by hydrogen and "mill annealed" structure of Ti6Al4V

4. Conclusions

The Ti6Al4V titanium alloy presents an excellent combination of the high strength/weight ratio combined with excellent mechanical and corrosion resistance. When coming in contact with hydrogen-containing environments, the titanium alloy can pick up massive amounts of hydrogen, especially at elevated temperatures. Hydrides precipitation within Ti6Al4V poses a major problem because it limits the potential applications and lifetime of airframe structures.

In this research, we have presented the influence of hydrogen diffusion on cracking propagation processes and on the formation of titanium hydrides types within the Ti6Al4V alloy along the intergranular path. Hydrogen was introduced electrochemically using a cathode charging system.

The H_2SO_4 (0.1 M) solution was used to accelerate the corrosion process of the titanium alloy, using two types of current density: J = 100 mA/cm^2 and J = 150 mA/cm^2. All samples immersed for more than 48 hours presented hydrides peaks when XRD analysis was performed and all had cracks in the cross-section, as shown by SEM and TEM analysis. It is thus recommended to introduce heat treatment or a coating process, which can be used to reduce hydrogen content in Ti alloys.

Acknowledgements. This work has been funded by the Politehnica University of Bucharest, through the "Excellence Research Grants" Program, UPB – GEX. Identifier: UPB–EXCELENȚĂ–2016, Nb. 29/26.09.2016.

References

[1] V.A.R. Henriques, P.P. de Campos, C.A.A. Cairo, and J.C. Bressiani, "Production of titanium alloys for advanced aerospace systems by powder metallurgy", *Mater. Res.* 8 (4), 443–446 (2005).

[2] R. Păcurar, N. Bâlc, and F. Prem, "Research on how to improve the accuracy of the SLM metallic parts", *AIP Conference Proceedings* 1353 (1), 1385–1390 (2011).

[3] C. Rontescu, D.T. Cicic, CG. Amza, O.R. Chivu, and G. Iacobescu, "Comparative analysis of the components obtained by additive manufacturing used for prosthetics and medical instruments", *Rev. Chim.* 68 (9), 2114–2116 (2017).

[4] M. Wachowski, L. Sniezek, I. Szachogluchowicz, R. Kosturek, and T. Plocinski, "Microstructure and fatigue life of Cp-Ti/316L bimetallic joints obtained by means of explosive welding", *Bull. Pol. Ac.: Tech.* 66 (6), 925–933 (2018).

[5] J. Maszybrocka, A. Stwora, B. Gapinski, G. Skrabalak, and M. Karolus, "Morphology and surface topography of Ti6Al4V lattice structure fabricated by selective laser sintering", *Bull. Pol. Ac.: Tech.* 65 (1), 85–92 (2017).

[6] I. Inagaki, T. Takechi, Y. Shirai and N. Ariyasu, "Application and features of titanium for the aerospace industry", *Nippon Steel & Sumitomo Metal Technical Report* 106, 22–27 (2014).

[7] J.J. Xu, H.Y. Cheung, and S.Q. Shi, "Mechanical properties of titanium hydride", *J. Alloys Compd.* 436 (1–2), 82–85 (2007).

[8] M. Ma, L. Wang, Y. Wang, W. Xiang, P. Lyu, B. Tang, and X. Tan, "Effect of hydrogen content on hydrogen desorption kinetics of titanium hydride", *J. Alloys Compd.* 709, 445–452 (2017).
[9] H. Numakura and M. Koiwa, "Hydride precipitation in titanium", *Acta Metall.* 32 (10), 1799–1807 (1984).
[10] H.J. Liu, L. Zhou, P. Liu, and Q.W. Liu, "Microstructural evolution and hydride precipitation mechanism in hydrogenated Ti–6Al–4V alloy", *Int. J. Hydrogen Energy* 34 (23), 9596–9602 (2009).
[11] Y. Baoguo, W. Yujie, Z. Yubin, and G. Longqing, "Hydrogenation behaviour of Ti6Al4V alloy", *Rare Metal Mat. Eng.* 46 (6), 1486–1490 (2014).
[12] D.O. Poletaev, D.A. Aksyonov, D.D. Vo, and A.G. Lipnitskii, "Hydrogen solubility in hcp titanium with the account of vacancy complexes and hydrides: A DFT study", *Comp. Mater. Sci.* 114, 199–208 (2016).
[13] C.P. Liang and H.R. Gong, "Fundamental influence of hydrogen on various properties of α-titanium", *Int. J. Hydrogen Energy* 35 (6), 3812–3816 (2010).
[14] A. San-Martin and F.D. Manchester, "The H-Ti (Hydrogen-Titanium) system", *Bull. Alloy. Phase Diagr.* 8 (1), 30–42 (1987).
[15] D.M. Wanderwalker, "The formation of hydrides in titanium", *Phys. Status Solidi A* 105 (2), 77–80 (1988).
[16] R. Laptev, V. Kudilarov, Y. Bordulev, A. Mikhaylov, and A.M. Lider, "Gas-phase hydrogenation influence on defect behavior in titanium-based hydrogen-storage material", *Prog. Nat. Sci-Mater.* 27 (1), 105–111 (2017).
[17] L. Miaoquan, Z. Weifu, Z. Tangkui, H. Hongliang, and L. Zhiqiang, "Effect of Hydrogen on Microstructure of Ti-6Al-4V Alloys", *Rare Metal Mat. Eng.* 39 (1), 1–5 (2010).
[18] P.A.T. Olsson, J. Blomqvist, C. Bjerken, and A.R. Massih, "Ab initio thermodynamics investigation of titanium hydrides", *Comp. Mater. Sci.* 97, 276–284 (2015).
[19] E.T. Gutelmacher and D. Eliezer, "The hydrogen embrittlement of titanium-based alloys", *JOM-US* 57 (9), 46–49 (2005).
[20] P. Muthukumar and M. Groll, "Metal hydride based heating and cooling systems: A review", *Int. J. Hydrogen Energy* 35 (8), 3817–3831 (2010).